ELSEVIER

Surface Science 412/413 (1998) 374–383

surface science

Formation of well-ordered surface compounds by coadsorption of thallium and bromide on the Au(111) electrode surface

J.X. Wang [a,*], I.K. Robinson [b], R.R. Adžić [a]

[a] *Chemical Science Division, Department of Applied Science, Building 815, Brookhaven National Laboratory, Upton, NY 11973, USA*
[b] *Department of Physics, University of Illinois at Urbana-Champaign, 1110 W Green Street, Urbana, IL 61801, USA*

Received 11 March 1998; accepted for publication 26 May 1998

Abstract

The structures of the adlayers formed on Au(111) in acid solution containing thallium and bromide have been investigated by using in situ surface X-ray diffraction. At the most positive potentials, where Br forms close-packed rotated-hexagonal monolayers, the surface is free of Tl. The Br adlayer disorders at the potential where thallium starts to coadsorb. With further decreasing potential, two well-ordered commensurate and one weakly-ordered incommensurate phases appear over a 0.7 V potential region prior to the formation of the close-packed rotated-hexagonal Tl monolayer. The structure factor analysis for the commensurate phases shows the formation of $TlBr_2$ and TlBr surface compounds in the 3-($\sqrt{13}\times\sqrt{13}$) and 2-($3\times\sqrt{3}$) phases, respectively. In addition, an adlayer-induced subsurface relaxation has been observed. Under the 2TlBr-($3\times\sqrt{3}$) adlayer, where bromide ions are at the bridge sites and thallium ions are situated near the hollow sites, the top layer of Au atoms displaces laterally along the $\sqrt{3}$ direction. This results in more uniform spacings between Tl and the three neighboring gold atoms, as well as an increase of the Br–Au separation.

Keywords: Bromide; Electrochemical methods; Surface relaxation and reconstruction; Surface structure; Thallium; X-ray scattering

1. Introduction

Coadsorption studies in surface science are important for understanding the reactivity of surfaces and are of particular relevance to electrochemistry where the electrode surfaces are in contact with cations, anions, and solvent molecules. Metal monolayers, formed by the so-called underpotential deposition (UPD), are strongly affected by coadsorbing anions. This has been known from early electrochemical [1] and radiotracer [2] studies. These systems are interesting because of new insights into fundamental questions of ordering of two-dimensional adlayers and because metal adatoms cause pronounced electrocatalytic effects [3]. Structures of such coadsorbed adlayers have recently been investigated with in situ atomic force microscopy [4,5], scanning tunneling microscopy (STM) [6–12], and surface X-ray scattering (SXS) techniques [13–19]. The UPD of Cu in the presence of sulfate, chloride, and bromide on Au and Pt surfaces attracted considerable attention. A variety of adlayer lattices, commensurate [6–11,15] or incommensurate [16,17], have been observed. These adlayers all consist of a bilayer with the cation directly contacting the substrate and the anion in the second

* Corresponding author. Fax: +1 516 2823137;
e-mail: jia@solids.phy.bnl.gov

0039-6028/98/$ – see front matter
PII: S0039-6028(98)00450-6

adlayer. The anion adsorption is enhanced due to a stronger interaction of the anions with the Cu than with the Au or Pt substrate. This, in turn, stabilizes the low-coverage Cu adlayers. An interesting counter example, with opposite distribution of anion and cation in the adlayer, is provided when alkali-metal cations coadsorb with iodide on Au(110) [20]. In this system, the anion interaction with the substrate is much stronger than that of the metal cation, causing the formation of coadsorbed adlayer with the anion chemisorbed on the substrate and the cation being coadsorbed.

In this paper, we report the results of electrochemical and SXS measurements of Tl–Br coadsorption on Au(111), where the cation–substrate, anion–substrate, as well as cation–anion interactions are comparable in strength over a wide potential region. Three mixed and two pure adlayer phases are formed at different potentials. Both the pure Br and pure Tl monolayers exhibit the same structural phase behavior within the potential regions of their existence as in the absence of the other species in solution. The Tl,Br/Au(111) system can be considered as a prototypical coadsorption system where the anion coverage decreases from the saturation value to zero, while the metal adatom coverage increases from zero to a full monolayer. Detailed structural information on Tl [13,14,21] and Br monolayers [22] on Au(111) can be found in previous publications. In this paper, we focus on the structure of the two well-ordered mixed commensurate phases. In these two phases, the first adlayer contains both Tl and Br. The structural phase behavior can be best understood in terms of the formation of surface compounds.

In addition, the top layer of the Au lattice was found to be distorted under the 2TlBr-$(3\times\sqrt{3})$ adlayer, which demonstrates significant interaction between the compound adlayer and the metal substrate. On semiconductor surfaces, where localized bonds are formed between adsorbate and substrate, subsurface relaxations involving lattice distortion in both lateral and vertical directions are often observed [23,24]. Because of the delocalized bonding, such effects are less common in metals, especially the non-transition metals [25]. It is hoped that the observation of lateral distortion reported in this paper will stimulate further studies of the phenomenon.

2. Experimental

The Au(111) crystal (miscut $<0.2^\circ$) was annealed in a propane flame before each experiment [26,27]. To prevent contamination from air, a drop of water was put onto the surface when the crystal cooled down to $\sim 100^\circ$C and kept there during the transfer to the X-ray electrochemical cell [28]. The solutions were prepared from Tl_2CO_3 and KBr (Aldrich), $HClO_4$ (Merck) and Milipore QC UV Plus water (Milipore Inc.). An outer chamber was filled with high purity nitrogen gas to prevent oxygen diffusing through the X-ray window during the measurements. A reversible hydrogen electrode in 0.1 M $HClO_4$ was used as a reference electrode.

X-ray measurements were performed at the beam line X22A with $\lambda = 1.20$ Å at the National Synchrotron Light Source. A four-circle diffractometer in a vertical scattering geometry was used. The symmetric $\omega = 0$ mode ensures that the incident and exit angles are held equal [29,30]. For convenience, a hexagonal coordinate system was used for the substrate crystal in which the reciprocal-space wave vector, $\boldsymbol{Q} = (a^*, b^*, c^*)\cdot(\boldsymbol{H}, \boldsymbol{K}, \boldsymbol{L})$, where $a^* = b^* = 4\pi/\sqrt{3}a$, $c^* = 2\pi/\sqrt{6}a$, $a = 2.885$ Å, and $\boldsymbol{L}$ is along the surface normal direction [28]. The intensities were measured by a NaI detector with a 2 mm × 2 mm slit located 650 mm from the sample. The resultant resolution in the surface plane ranges from 0.01 to 0.02 $Å^{-1}$ (full width at half maximum), which is larger than the intrinsic peak width for all the reflections where the integrated intensity was acquired. The structure factors were obtained after correcting the integrated intensities for the variation of the Lorentz factor, the effective sample area, and the resolution along the surface normal direction [31].

3. Results and discussion

3.1. Voltammetry and structural phase transitions

The voltammetry curve for the underpotential deposition of Tl on Au(111) in 0.1 M $HClO_4$

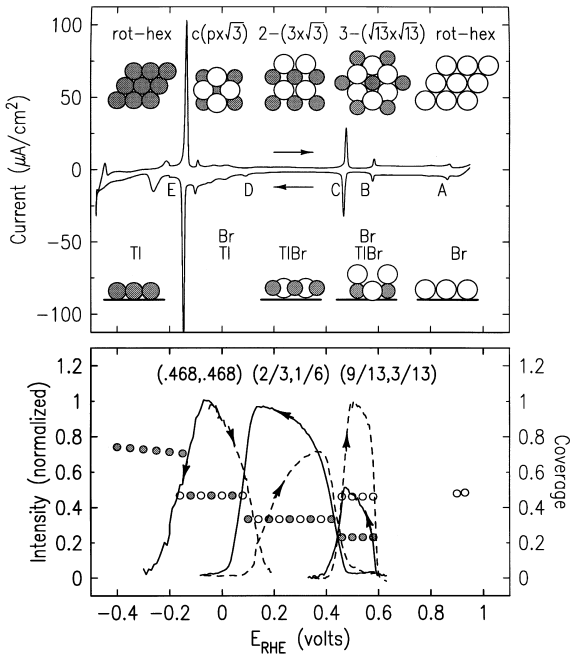

Fig. 1. (Top) Voltammetry curve for the UPD of Tl on Au(111) in 0.1 M $HClO_4$ containing 1 mM TlBr. Sweep rate 20 mV/s. The in-plane and surface normal structural models are deduced from the surface X-ray diffraction measurements. (Bottom) Potential dependent diffraction intensities at the indicated positions for the three coadsorbed phases. Scan rate 0.5 mV/s, except for the $c(2.14\times\sqrt{3})$ phase at (0.468, 0.468), where it is 0.2 mV/s, started after holding the potential around -0.1 V for several hours. Coverages, in units of monolayers of the Au substrate, shown by the open and filled circles for Br and Tl, respectively, are calculated from the adlayer lattice constants.

solution containing 1 mM TlBr (Fig. 1) shows a multitude of reversible peaks over a wide potential region. These peaks are ascribed to the effect of Br^- coadsorption on the UPD of Tl since they do not appear in the absence of Br^-. Decreasing the sweep rate does not provide a better resolution. Bromide, at potentials positive of peak A, forms a close-packed, rotated-hexagonal adlayer as in the absence of Tl^+ in solution [22]. Likewise, thallium forms a close-packed, rotated-hexagonal adlayer at potentials negative of peak E as in the absence of Br^- [13,14,21]. At the intermediate potentials, three superlattice structures, which do not exist in the absence of either Tl^+ or Br^-, are observed. The structural models shown in Fig. 1 are derived from the surface X-ray scattering measurements described in this paper. The van der Waals diameter for Br (open circle) of 3.92 Å [32] is used in all the proposed models since the ionic diameter of Br^- has almost the same value. Thallium (shaded circles), however, has diameters of 3.456 and 2.98 Å in the rotated hexagonal phase and the three coadsorbed phases, respectively. The first is the metallic nearest neighbor separation in the bulk crystal and the second is the ionic diameter of Tl^+ [32].

Coverages for Tl and Br in the ordered phases, derived from the adlayer lattice structures, together with the potential-dependent diffraction intensities for the three coadsorbed phases are shown in the lower panel of Fig. 1. The Tl coverage decreases with increasing potential in the rotated-hexagonal phase and upon each phase transition, while the bromide coverage is almost a constant at potentials positive of -0.2 V. At potentials between peaks B and A, no long range ordering is found and the constant current level suggests a gradual desorption of Tl over this potential region.

The phase transitions are identified by the variation of diffraction intensities during the negative (solid line) and positive (dashed line) potential scans at (9/13, 3/13), (2/3, 1/6), and (0.468, 0.468) positions for the $(\sqrt{13}\times\sqrt{13})$, $(3\times\sqrt{3})$ and $c(2.14\times\sqrt{3})$ phases, respectively (Fig. 1). The rising and falling intensities indicate the formation and disappearance of the corresponding phases. The first two phases are commensurate and well-ordered, existing in the low-current potential regions between the current peaks B–C and C–D. In contrast to the reversible current peaks B and C observed with a sweep rate of 20 mV/s, diffraction intensities from the $(\sqrt{13}\times\sqrt{13})$ and $(3\times\sqrt{3})$ adlayer exhibit significant hysteresis even at a sweep rate of 0.5 mV/s. The maximum intensity is higher in the positive direction for the $(\sqrt{13}\times\sqrt{13})$ phase, but in the negative scan direction for the $(3\times\sqrt{3})$ phase. This is due in part to the thin layer geometry of the X-ray cell, and also in part to the slow kinetics of the ordering which involves the lateral relaxation of gold surface atoms (see Section 3.3). The coherence length of these two adlayers is found, by using Soller slits, to be at least 400 Å, as calculated from 2π divided

by the in-plane radial peak full width at half maximum.

The diffraction observed at the (0.468, 0.468) position is broad and weak, but the peak does not shift with potential. This is the only peak observed in an extensive search in reciprocal space at the potentials between the current peaks D and E. The proposed structural model has a $c(2.14\times\sqrt{3})$ unit cell containing two Tl ions in the first adlayer and two Br ions in the second adlayer. The first order diffractions (not observed) are expected to be weaker than the second order diffraction at (0.468, 0.468). This is because the scattering from Tl and Br is out of phase for the former, but in phase for the latter. The fact that only the lowest order in-phase diffraction can be observed, and that the peak is significantly broader than those in the other two mixed adlayers, suggests that there is very limited ordering in this phase. Thus, the coverage calculated from the lattice may differ from the average coverage over a large area of the surface. The structure along the surface normal direction has not been determined for this phase.

3.2. The $3TlBr_2$-$(\sqrt{13}\times\sqrt{13})$ phase

At 0.55 V, in-plane diffractions were observed at the non-integer index positions corresponding to a 3-$(\sqrt{13}\times\sqrt{13})$ hexagonal lattice as shown by the dashed line in Fig. 2b. The primitive unit cell (solid line) is also hexagonal and the lattice constant equals $\sqrt{13}/\sqrt{3}$ times the gold lattice constant, or 6.006 Å. The θ-rocking curves of the two lowest-order in-plane diffraction peaks are shown in Fig. 2a. The second order peak at (9/13, 3/13) is much stronger than the first order peak at (2/13, 5/13), which suggests that there are at least two atoms in the primitive unit cell. In order to determine the chemical components in this phase, the structure factor intensity has been measured for 10 in-plane peaks ($L=0.2$) as shown by the areas of the open circles in the inset to Fig. 2a.

Fig. 3 shows the measured structure factor intensities and the fits based on the TlBr and $TlBr_2$ models depicted in Fig. 2b and c, respectively. The data are indexed by using the primitive adlayer unit cell as the basis, and the error bars show the

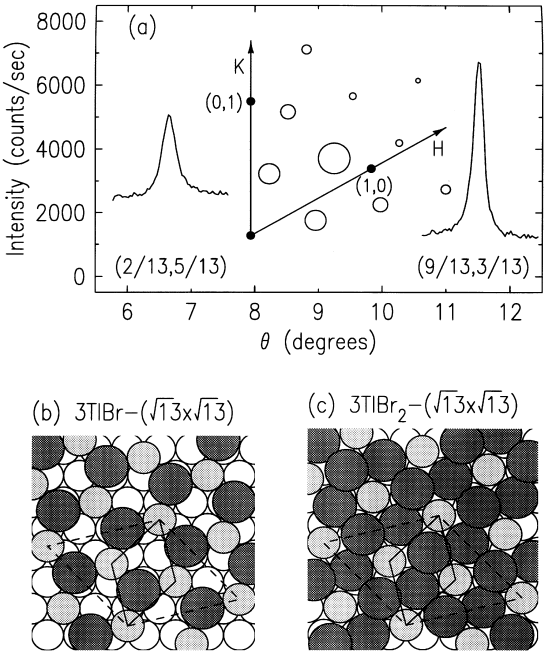

Fig. 2. (a) In-plane θ-rocking scans at (2/13, 5/13, 0.2) and (9/13, 3/13, 0.2) positions measured at 0.55 V for the first and second order diffractions from the $(\sqrt{13}\times\sqrt{13})$ phase. Inset: Observed in-plane diffraction peaks from the adlayer (open circles) and the Au(111) substrate (filled circles). The areas of the open circles are proportional to the measured structure factor intensities. Only one of the two symmetry equivalent domains is shown for simplicity. (b) Structural model for the first adlayer containing three Tl (light shade, 2.98 Å) and three Br (heavy shade, 3.92 Å) in the $(\sqrt{13}\times\sqrt{13})$ unit cell. (c) In-plane projection of the first (TlBr) and the second (Br) adlayers. The positions of Tl and Br with respect to the Au(111) substrate are for illustration only since they are not determined in our study.

deviation of the values obtained from symmetry equivalent spots. In the TlBr model, bromide ions are assumed to be in the hollow sites of the hexagonal Tl adlayer with a negligible layer spacing between Tl and Br because the sum of ionic radii of bromide (1.96 Å) and thallium (1.49 Å) [32], 3.45 Å, is very close to the in-plane Tl–Br spacing of 3.47 Å. Since six-fold symmetry of the diffraction was observed, it is assumed that bromide ions can be in either of the possible triangular sites in Fig. 2b with equal probability, so the calculated intensities for both cases are averaged. The lateral root-mean-square displacement amplitudes (σ_{xy}) of Tl and Br are allowed to vary. The

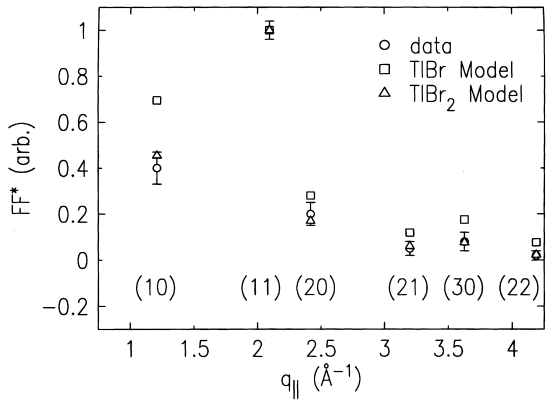

Fig. 3. Structural factor intensities of the in-plane diffraction peaks (indexed by using the primary adlayer unit cell as the basis) compared with the calculated values for the $(\sqrt{13}\times\sqrt{13})$ phase using the TlBr and $TlBr_2$ models.

failure of the TlBr model is demonstrated by the large deviation of the fit (squares) from the data. A better fit (triangles) is obtained with the $TlBr_2$ model, in which both triangular sites are occupied by bromide ions as shown in Fig. 2c. This model has three free parameters which are least-squares fit to five independent data points. The resulting $\chi^2=0.52$, indicating a disagreement which is at the level of the measurement uncertainties themselves.

The bromide ions in the $TlBr_2$ phase are likely to be in two different layers because the in-plane nearest neighbor separation (3.47 Å) is too small compared with the diameter of bromide (3.92 Å). This is confirmed by analyzing the specular reflectivity data discussed in the next paragraph. Using the layer spacings (d_z) and vertical root-mean-square displacement amplitudes (σ_z) obtained from

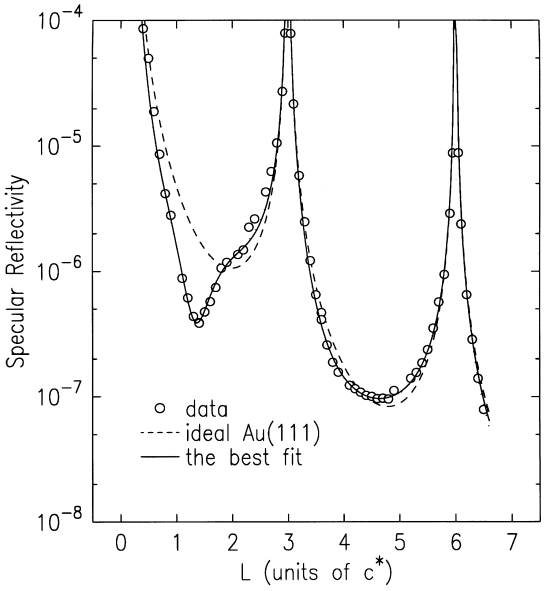

Fig. 4. Specular reflectivity profiles obtained from $3TlBr_2$-$(\sqrt{13}\times\sqrt{13})$/Au(111) in 0.1 M $HClO_4$ containing 1 mM TlBr at 0.55 V.

specular reflectivity analysis (either set in Table 1), the best fit to the in-plane diffraction intensities, as shown in Fig. 3, is obtained by varying σ_{xy} for each of the three adlayers. As also listed in Table 1, the σ_{xy} values for Tl (0.48 Å) and the first Br (0.70 Å) adlayer are rather high. This probably represents static, rather than dynamic disorder of the adlayer because neither Tl nor Br can occupy high-symmetry site on the Au(111) substrate in this phase.

The specular reflectivity for the $(\sqrt{13}\times\sqrt{13})$

Table 1
Parameters obtained from analysis of specular reflectivity and in-plane diffraction intensities (last column)

	First set		Second set		
Atom	d_z^a (Å)	σ_z^b (Å)	d_z^a (Å)	σ_z^b (Å)	σ_{xy}^c (Å)
Tl	3.01 ± 0.07	0.10 ± 0.03	2.69 ± 0.03	0.18 ± 0.06	0.48 ± 0.02
Br	2.65 ± 0.11	0.46 ± 0.13	3.39 ± 0.06	0.18 ± 0.14	0.70 ± 0.02
Br	6.79 ± 0.19	0.86 ± 0.18	6.73 ± 0.16	0.83 ± 0.18	0.5 ± 0.4

[a] Spacing between the referred adlayer and the top layer of the Au(111) substrate.
[b] Vertical root-mean-square displacement amplitude.
[c] Lateral root-mean-square displacement amplitude, determined from the in-plane analysis while the d_z and σ_z were held fixed at the values in either set of parameters obtained from analysis of the specular reflectivity.

phase is shown in Fig. 4. The dashed line is the calculated curve for an ideal Au(111) crystal, and the solid line is the best fit to the data using the structural model containing one Tl and two Br adlayers. The coverage for each layer is fixed at 0.23 (=3/13), while the distance from the Au(111) surface and the vertical root-mean-square displacement amplitude for each adlayer are allowed to vary. Two sets of parameters, which yield nearly identical curves, are listed in Table 1. It is not clear which set of parameters is more reasonable, i.e. whether the first Br adlayer should be at a slightly lower (the first set) or higher position (the second set) than the Tl adlayer since the adlayer spacings are not necessarily proportional to their ionic sizes. The layer spacings of pure Tl and Br on Au(111) have been found to be 2.66 [13,14] and 2.33 Å [28], respectively, which are consistent with the values calculated from covalent radii. Despite the uncertainty in the layer spacings for the Tl and the first Br adlayers, both parameter sets indicate that the second Br adlayer is at least 3 Å above the Tl and the first Br adlayer. At such a distance, Br interaction with Au is very weak. Apparently, the adsorption and ordering of the second Br adlayer are mainly due to the ionic interaction between the adsorbates. It is likely that at these very positive potentials the positive partial charge on Tl is larger than the negative partial charge on Br. This results in the $TlBr_2$ stoichiometry. From these analyses, the atomic coverages for Tl (3/13 = 0.23) and Br ($0.23 \times 2 = 0.46$) are obtained. The latter is close to the Br coverage of 0.48 in the rotated-hexagonal phase at 0.9 V, consistent with the rotating disk–ring result that no significant desorption of Br occurs at potentials above −0.1 V [33].

3.3. The 2TlBr-($3 \times \sqrt{3}$) phase

In the potential region between 0.45 and 0.10 V, the 2TlBr-($3 \times \sqrt{3}$) phase is formed. The in-plane diffraction peaks observed from one of the three symmetry equivalent domains are shown in Fig. 5b. Ignoring for the moment the peak at (1/3, 5/6), the diffraction pattern can be indexed by the basis vectors (2/3, −1/3) and (0, 1/2) which

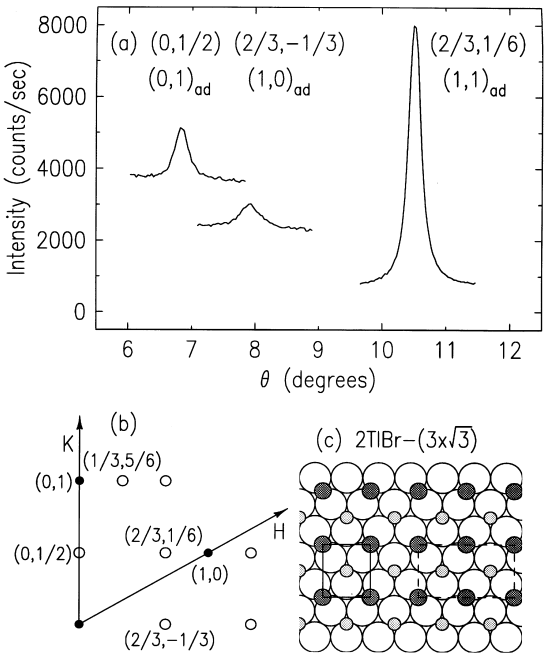

Fig. 5. (a) In-plane θ-rocking scans ($L = 0.2$) through the three low order diffractions from the 2TlBr-($3 \times \sqrt{3}$) adlayer at 0.25 V. (b) Observed in-plane diffraction peaks from the adlayer (open circles) in one of the three symmetry equivalent domains and the Au(111) substrate (filled circles). (c) Structural model for the ($3 \times \sqrt{3}$) phase with two Tl (lightly shaded) and two Br (heavily shaded) in the unit cell. The registry with the Au(111) surface is determined from analysis of the data shown in Fig. 6.

correspond to a primitive ($1.5 \times \sqrt{3}$) rectangular unit cell (solid line in Fig. 5c). Using this adlayer unit cell, the basis vectors (2/3, −1/3) and (0, 1/2) can be renamed as $(1, 0)_{ad}$ and $(0, 1)_{ad}$, respectively. As shown in Fig. 5a, the (2/3, 1/6), or $(1, 1)_{ad}$, peak is much more intense than the other two lower order peaks. This is the characteristic of a centered structure shown in Fig. 5c, in which Br and Tl are at the corners and in the center of the ($1.5 \times \sqrt{3}$) unit cell, respectively. In a mixed centered structure, the first order peaks have structure factors which are the difference of the form factors of the two atom types. The second order peak $(1, 1)_{ad}$ is given by the sum of the two form factors.

The ($1.5 \times \sqrt{3}$) unit cell discussed so far is not compatible with the translational symmetry of the substrate. One of the two atom types, at the corner

of the cell, can align with successive bridge sites of the substrate, but the other does not fall at a special position. The nearest hollow site is a short distance above or below the center position, alternating from one cell to the next. The structure that utilizes these alternating hollow sites is the p2mg($3\times\sqrt{3}$) unit cell drawn as the dashed box in Fig. 5c. After testing several versions of this model (see below), we found it worked better with Br ions at the bridge sites and Tl ions near to the hollow sites. The selection rules for the diffraction from a p2mg structure allow some "half order" reflections such as the $(1/2, 2)_{ad}$ peak at (1/3, 5/6). The fact that the diffraction intensity is detectable at $(1/2, 2)_{ad}$ indicates that either the two thallium ions move in the opposite directions towards the hollow sites, and/or the underlying gold atoms displace from the lattice sites to adjust to the presence of the Tl.

Further measurements were made of the first three surface rods, i.e. the L dependence of reflections at $(1, 0)_{ad}$, $(0, 1)_{ad}$, and $(1, 1)_{ad}$ positions. The diffraction intensities at these positions are from one of the three symmetry equivalent domains. The $(2, 0)_{ad}$ and $(1, 2)_{ad}$ rods, however, cannot be measured separately because the $(2, 0)_{ad}$ diffraction from one domain overlaps in the in-plane reciprocal space with the $(1, 2)_{ad}$ diffraction from the other two $\pm 120^{\circ}$ rotated domains. The data of the three lowest order rods are shown in Fig. 6a and analyzed by using a structural model containing six Au, two Tl, and two Br atoms in a $(3\times\sqrt{3})$ unit cell. The fact that the $(1, 1)_{ad}$ is always more intense than the other two over the large range of L indicates that Tl and Br have similar heights above the gold surface. The first calculation is made by assuming that all the atoms are at the ideal lattice sites (see Fig. 6b) and have a σ_{xy} value of 0.1 Å. With the same intensity conversion factor, it produces the correct intensity levels for all three rods (dashed lines).

It can be seen that the rod data oscillate with respect to the dashed lines. These oscillations can only be attributed to the interference from different layers, hence, the displacement of Au atoms is ascertained. Since the oscillation of the $(1, 0)_{ad}$ rod is absent or very weak, the displacements must

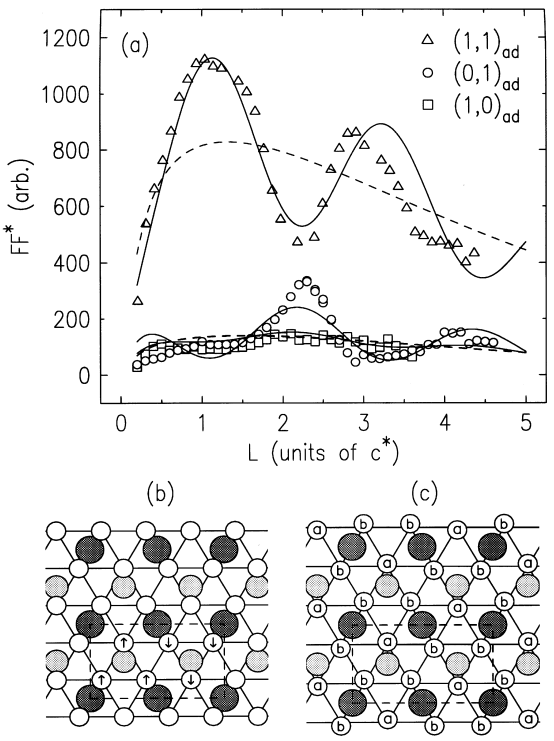

Fig. 6. (a) Surface rods measured for the $(3\times\sqrt{3})$ phase at 0.25 V. The decrease of intensity at small L is partly due to the X-ray absorption by the thin layer solution which is included in the calculation. The solid (dashed) lines are the fits with (without) the displacement of the top layer Au atoms. (b and c) In-plane structural models for 2TlBr-($3\times\sqrt{3}$) on Au(111). Heavily and lightly shaded circles represent Br and Tl, respectively. Open circles represent the top layer of Au atoms which are at the ideal lattice sites in (b), but displaced in (c). The arrows in (b) show the directions of the displacements, and the Au atoms with a displacement of 0.17 and 0.24 Å are labeled as "a" and "b" in (c), respectively.

be essentially perpendicular to the x-axis or the close-packed rows of Au(111). A simple model, in which the close-packed Au rows pair up, was tested first. This model was found inadequate because it does not yield the oscillation in the $(1, 1)_{ad}$ rod.

The solid lines show the best fits obtained by using a structural model where bromide ions are at the bridge sites and the Au atoms displace laterally from the regular lattice sites (see Fig. 6c). Other models fail to reproduce a correct phase relationship between the oscillations in the $(0, 1)_{ad}$ and $(1, 1)_{ad}$ rods. For example, interchang-

ing Tl and Br will cause the calculated oscillation to be out of phase with the measured $(0, 1)_{ad}$ rod. Five parameters are allowed to vary in fitting. The Tl–Au and Br–Au layer spacings are both 3.2 Å, basically determined by the oscillation frequency. The y-axis displacements of the "a" and "b" type Au atoms are 0.17 and 0.24 Å, respectively (see Fig. 6c). They are mainly determined by the amplitude of the oscillations in the $(0, 1)_{ad}$ and $(1, 1)_{ad}$ rods and are all in a direction to accommodate the 0.42 Å misfit between the center of the $(1.5 \times \sqrt{3})$ unit cell and the hollow site of the underlying substrate. The fifth parameter is the x-axis displacement of the "b" type Au atoms, which is found to be very small (0.03 Å) and not shown in Fig. 6c.

The fits cannot be improved by adding displacements along the surface normal direction for the top layer Au or by allowing σ to vary for the involved layers. Adding displacements of Tl ions from the center of the rectangular lattice in the model has little effect on these surface rods. In principle, the (1, 0) and (0, 1) substrate truncation rods are more sensitive to the displacement of adatoms [31,34]. However, the effect of a 0.1 Å displacement of Tl is small and we do not have data accurate enough to determine whether or not such a displacement occurs in addition to the Au displacements. A model including several relaxed Au layers appear to be needed for improving the fits to the surface rods. It has been shown for semiconductor surfaces that the adsorbate-induced subsurface relaxation can extend up to four atomic layers into the bulk [23,24]. The modeling of such a system, however, turns out to be rather complicated due to the lack of a simple symmetry. The displacements found by using the model including only the top layer of Au should be considered to be the best to date.

3.4. Structure-determining interactions

Substrate–adsorbate interaction apparently plays an important role in the formation of the two commensurate phases. The influence of the Au(111) periodic potential is strong since the 3-$(\sqrt{13} \times \sqrt{13})$ and 2-$(3 \times \sqrt{3})$ phases are also observed for chloride as the coadsorbed anion. In the 3-$(\sqrt{13} \times \sqrt{13})$ phase, chloride ions, which are smaller than bromide ions, may all be in the same layer with Tl. The fact that the in-plane lattice is not expanded in the $TlBr_2$ adlayer, but the bromide ions are placed in two layers, indicates the importance of the commensuration. In contrast, CuCl and CuBr have been found to form incommensurate, aligned hexagonal bilayers on Pt(111) in which the lattice constant changes with the size of the anion [16,17].

The phase transition from the quasi-square TlBr phase to the hexagonal $TlBr_2$ phase with increasing potential can be understood in terms of the potential dependence of partial charge on the adsorbates. The very low capacitance current in the potential region of the $(3 \times \sqrt{3})$ and $(\sqrt{13} \times \sqrt{13})$ phase suggests that the charge is near zero for the whole adlayer in these two phases. The stoichiometry, therefore, should be inversely proportional to the ratio of the partial charges on the species. For the 2TlBr-$(3 \times \sqrt{3})$ phase, formed in the middle potential region, the positive charge on Tl is probably about the same as the negative charge on Br. The adlayer exhibits a quasi-square symmetry because it allows each ion to surround itself with the maximum number of counterions with about equal absolute charge. Other binary ionic adlayers, e.g. CsI, KI, NaI, and LiI, have been found to form uniaxially commensurate lattices with quasi-square symmetry on Au(110) [20]. The positive charge on metal adsorbates increases and the negative charge on adsorbed halides decreases with increasing potential. This leads to a phase transition involving a change of stoichiometry from TlBr to $TlBr_2$ and a lattice symmetry change from quasi-square to hexagonal.

The physical origin for the Au surface relaxation induced by the 2TlBr-$(3 \times \sqrt{3})$ adlayer, though not fully understood yet, can be explained to some extent by the structural model proposed. The displacements of the top layer of gold atoms, as seen by comparing Fig. 6c with Fig. 6b, result in more uniform Tl–Au spacings and also an increase of the Br–Au separation. The overall consequence suggests that the Au surface relaxation originates from the lattice misfit between the substrate and

adlayer, i.e. the center of the adlayer primitive unit cell does not align exactly with the preferred three-fold hollow sites on Au(111). The symmetry pattern of the displacements is such that it reduces this misfit. The increase of the Br–Au separation may be a beneficial coincidence because the larger displacement of the "b" type atoms compared to that of the "a" type atoms can be explained by assuming that the increase of Au–Br nearest neighbor separation is favorable.

This mechanism differs distinctly from those for semiconductor surfaces where the adsorption is site specific involving localized covalent bonding and the subsurface relaxation occurs when the total energy is minimized by the change of the bond lengths and/or angles [35,36]. On metals, especially non-transition metals, delocalized bonding is present and the influence of substrate periodic potential on the adlayer structure is often more important. For example, the substrate-induced spatial modulation of the incommensurate Tl monolayer on Ag(111) has been reported [34]. Due to the misfit between adlayer and substrate lattices, some thallium ions will be at the less favorable sites, so that they displace from the ideal adlattice sites in order to have more favorable surface geometry. Generally speaking, the energetic cost for adatoms to displace should be lower than that for substrate atoms because the latter would create another misfit between the relaxed top layer and the layer below. Therefore, the substrate-induced spatial modulation in adlayers is easily understood. The same argument raises a question as to why the Au surface relaxation, instead of Tl displacement, occurs in the case of TlBr on Au(111). There is a possible explanation from the structural point of view. Note that in the $(3\times\sqrt{3})$ adlayer, Tl and Br are approximately in the same plane and their separation, 3.31 Å, is slightly smaller than the sum of the ionic radii (3.45 Å). In such a compressed and commensurate adlayer, Tl displacement would be more difficult than in the incommensurate Tl monolayer. Subsurface relaxation then turns out to be more favorable. The nature of the chemical bonding must also play a role in the observed subsurface relaxation. Further studies are required for a better understanding of the adlayer-induced lateral lattice distortion at metal surfaces.

4. Conclusions

The electrochemical and X-ray diffraction measurements presented here show that Tl–Br co-adsorption occurs over a wide potential region with distinct structural phases occurring at different potentials. From the analysis of in-plane fractional-order diffraction intensities and of specular reflectivity, two bromides per Tl are found in the 3-$(\sqrt{13}\times\sqrt{13})$ phase with one Br within and the other above the Tl adlayer. At more negative potentials, the 2TlBr-$(3\times\sqrt{3})$ phase is identified. The ratio of the partial charges on Tl and Br is likely to be the most important factor in determining the stoichiometry and adlattice symmetry. The registry of the adsorbates in the 2TlBr-$(3\times\sqrt{3})$ phase and the lateral displacements of the top layer of Au atoms are determined from the analysis of fractional-order rods. This adlayer-induced subsurface relaxation results in more uniform spacings between Tl and the three neighboring gold atoms, as well as an increase of the Br–Au separation. This phenomenon of surface response to an overlayer is similar to those observed from semiconductor surfaces [23,24], and demonstrates an active role of the substrate atomic structure in formation of surface compounds on metal electrode surfaces.

Acknowledgements

The authors thank B.M. Ocko and S. Feldberg for useful discussions. This research was performed under the auspices of the US Department of Energy, Divisions of Chemical and Materials Sciences, Office of Basic Energy Sciences under Contract No. DE-AC02-98CH10886. IKR acknowledges support from the Department of Energy under Contract DEFG02-96ER45439.

References

[1] D.M. Kolb, in: H. Gerischer, C.W. Tobias (Eds.), Advances in Electrochemistry and Electrochemical Engineering, vol. 11, Wiley-Interscience, New York, 1978, p. 125.
[2] G. Horanyi, G. Vertes, J. Electroanal. Chem. 55 (1974) 45.
[3] R.R. Adžić, in: H. Gerischer, C.W. Tobias (Eds.), Advances in Electrochemistry and Electrochemical Engineering, vol. 13, Wiley-Interscience, New York, 1984, p. 159.
[4] S. Manne, P.K. Hansma, J. Massie, V.B. Elings, A.A. Gewirth, Science 251 (1991) 183.
[5] C.-H. Chen, A.A. Gewirth, J. Am. Chem. Soc. 114 (1992) 5439.
[6] O.M. Magnussen, J. Hotlos, R.J. Nichols, D.M. Kolb, R.J. Behm, Phys. Rev. Lett. 64 (1990) 2929.
[7] O.M. Magnussen, J. Hotlos, G. Beitel, D.M. Kolb, R.J. Behm, J. Vac. Sci. Technol. B9 (1991) 969.
[8] K. Sashikata, N. Furuya, K. Itaya, J. Electroanal. Chem. 316 (1991) 275.
[9] W. Haiss, D. Lackey, J.K. Sass, H. Meyer, R.J. Nichols, Chem. Phys. Lett. 200 (1992) 343.
[10] F.A. Moller, O.M. Magnussen, R.J. Behm, Phys. Rev. B 51 (1995) 2484.
[11] F. Moller, O.M. Magnussen, R.J. Behm, Electrochim. Acta 40 (1995) 1259.
[12] H. Matsumoto, J. Inukai, M. Ito, J. Electroanal. Chem. 379 (1994) 223.
[13] J.X. Wang, R.R. Adžić, B.M. Ocko, J. Phys. Chem. 98 (1994) 7182.
[14] R.R. Adžić, J.X. Wang, W. Polewska, B.M. Ocko, Electrochim. Acta 40 (1995) 83.
[15] M.F. Toney, J.N. Howard, J. Richer, G.L. Borges, J.G. Gordon, O.R. Melroy, D. Yee, L.B. Sorensen, Phys. Rev. Lett. 75 (1995) 4472.
[16] I.M. Tidswell, C.A. Lucas, N.M. Marković, P.N. Ross, Phys. Rev. B 51 (1995) 10205.
[17] C.A. Lucas, N.M. Marković, I.M. Tidswell, P.N. Ross, Physica B 221 (1996) 245.
[18] R.R. Adžić, J.X. Wang, O.M. Magnussen, B.M. Ocko, J. Phys. Chem. 100 (1996) 14721.
[19] C.A. Lucas, N.M. Marković, P.N. Ross, Langmuir 13 (1997) 5517.
[20] J.X. Wang, G.M. Waston, B.M. Ocko, J. Phys. Chem. 100 (1996) 6672.
[21] M.F. Toney, J.G. Gordon, M.G. Samant, G.L. Borges, O.R. Melroy, D. Yee, L.B. Sorensen, J. Phys. Chem. 99 (1995) 4733.
[22] O.M. Magnussen, B.M. Ocko, J.X. Wang, R.R. Adžić, J. Phys. Chem. 100 (1996) 5500.
[23] J.S. Pedersen, R. Feidenhans'l, M. Nielsen, K. Kjaer, F. Grey, R.L. Johnson, Surf. Sci. 189/190 (1987) 1047.
[24] C. Kim, D.A. Walko, I.K. Robinson, Surf. Sci. 388 (1997) 242.
[25] G.A. Somorjai, M.A. Van Hove, Acta Crystallogr. B51 (1995) 502.
[26] J. Clavilier, R. Faure, G. Guinet, R. Durand, J. Electroanal. Chem. 107 (1980) 205.
[27] J. Wiechers, T. Twomey, D.M. Kolb, R.J. Behm, J. Electroanal. Chem. 248 (1988) 451.
[28] J. Wang, B.M. Ocko, A.J. Davenport, H.S. Isaacs, Phys. Rev. B 46 (1992) 10321.
[29] W.R. Busing, H.A. Levy, Acta Crystallogr. 22 (1967) 457.
[30] S.G.J. Mochrie, J. Appl. Cryst. 21 (1988) 1.
[31] I.K. Robinson, in: D.E. Moncton, G.S. Brown (Eds.), Handbook on Synchrotron Radiation, vol. 3, North-Holland, Amsterdam, 1991, p. 221.
[32] J. Emsley, The Elements, Clarendon Press, Oxford, 2nd edn., 1991.
[33] R.R. Adžić, J.X. Wang, J. Phys. Chem., in press.
[34] M.F. Toney, J.G. Gordon, M.G. Samant, G.L. Borges, O.R. Melroy, L.S. Kau, D.G. Wiesler, D. Yee, L.B. Sorensen, Phys. Rev. B 42 (1990) 5594.
[35] J.E. Jaffe, P. Zapol, Surf. Sci. 381 (1997) L563.
[36] V. Kairys, J.D. Head, Surf. Sci. 380 (1997) 283.